iScience

CellPress

Article

MORC3 Forms Nuclear Condensates through Phase Separation

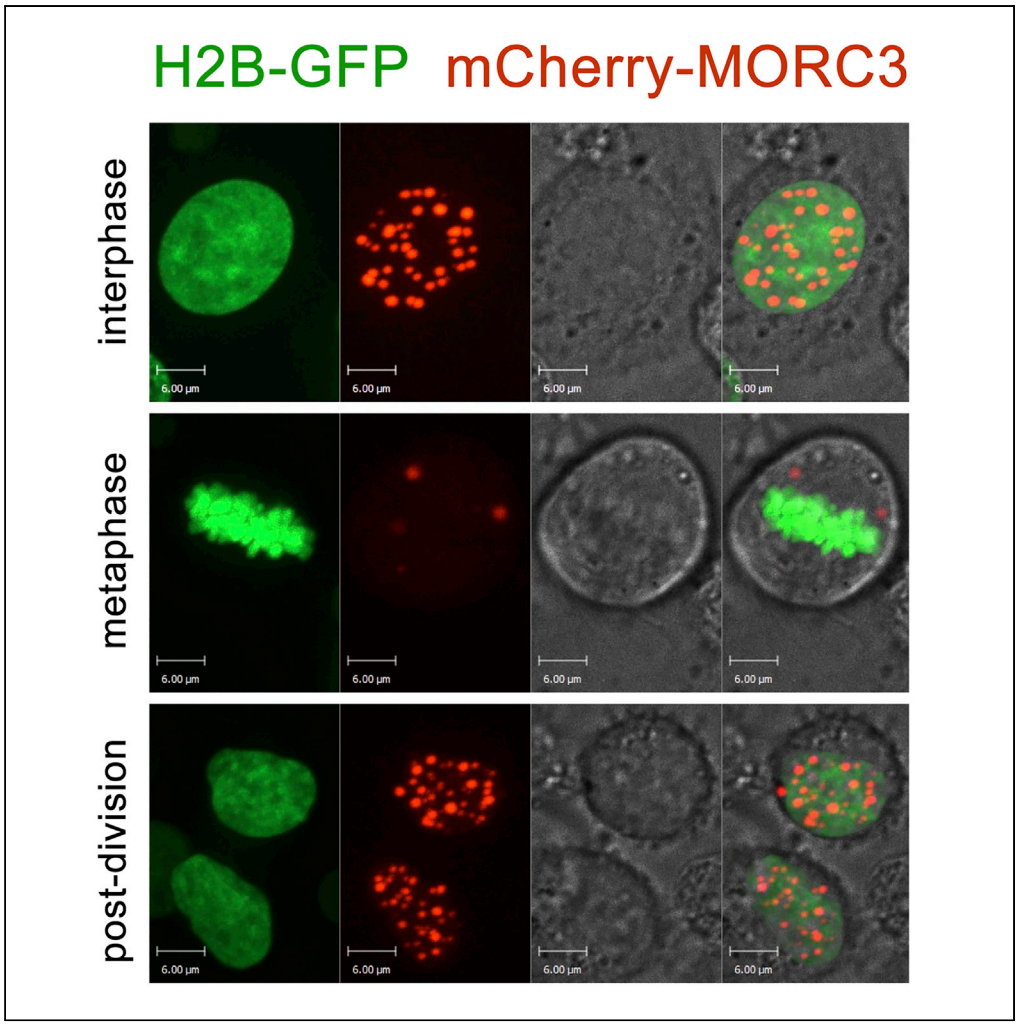

Yi Zhang, Bianca Bertulat, Adam H. Tencer, ..., Joshua Black, M. Cristina Cardoso, Tatiana G. Kutateladze

tatiana.kutateladze@ucdenver.edu

HIGHLIGHTS

MORC3 forms nuclear condensates with liquid-like characteristics

Morphology of the MORC3 condensates changes during the cell cycle

Phase separation depends on the MORC3 ATPase activity and DNA binding

CW impedes the ability of MORC3 to form condensates

Zhang et al., iScience *17*, 182–189
July 26, 2019
https://doi.org/10.1016/j.isci.2019.06.030

iScience

CellPress

Article

MORC3 Forms Nuclear Condensates through Phase Separation

Yi Zhang,[1] Bianca Bertulat,[2] Adam H. Tencer,[1] Xiaojun Ren,[3] Gregory M. Wright,[1] Joshua Black,[1] M. Cristina Cardoso,[2] and Tatiana G. Kutateladze[1,4,*]

SUMMARY

Phase separation can produce local structures with specific functionality in the cell, and in the nucleus, this can lead to chromatin reorganization. Microrchidia 3 (MORC3) is a human ATPase that has been implicated in autoimmune disorders and cancer. Here, we show that MORC3 forms phase-separated condensates with liquid-like properties in the cell nucleus. Fluorescence live-cell imaging reveals that the MORC3 condensates are heterogeneous and undergo dynamic morphological changes during the cell cycle. The ATPase activity of MORC3 drives its phase separation *in vitro* and requires DNA binding and releasing the MORC3 CW domain-dependent autoinhibition through association with histone H3. Our findings suggest a mechanism by which the ATPase function of MORC3 mediates MORC3 nuclear compartmentalization.

INTRODUCTION

Microrchidia 3 (MORC3) ATPase is associated with a number of human diseases, including autoimmune disorders, Down syndrome, cancer, and viral infection (Andrews et al., 2016; Gonzalez-Fernandez et al., 2012; Gunawardena et al., 2009; Li et al., 2016; Sloan et al., 2016; Ver et al., 2015). This multi-modular enzyme contains an N-terminal ATPase-CW cassette followed by a long and largely unstructured C-terminal region, harboring at least one coiled-coil and several SUMOylation sites. MORC3 exists in autoinhibited and active states, and the mechanism underlying the state transition has recently been elucidated (Andrews et al., 2016; Zhang et al., 2019a). A tight binding of the CW domain to the adjacent catalytic ATPase domain impedes the ATPase domain's association with DNA necessary for the catalytic activity of MORC3, resulting in MORC3 autoinhibition. Competitive binding of the CW domain to histone H3, particularly methylated at lysine 4 (H3K4me), frees the ATPase domain for the interaction with DNA, alleviating autoinhibition. The influenza virus A protein NS1, which contains the amino acid sequence similar to that of histone H3K4me, has also been shown to activate MORC3, evading anti-viral immune response (Zhang et al., 2019b).

In cells, both endogenous and overexpressed MORC3 forms nuclear bodies (NBs) in promyelocytic leukemia protein (PML)-dependent and PML-independent manner (Andrews et al., 2016; Mimura et al., 2010). The number of PML-independent MORC3-NBs appears to vary among cell types, accounting for only 5% in mouse embryonic fibroblasts but making up 70%–85% in mouse bone marrow, solenocytes, and CD11b$^+$ cells (Mimura et al., 2010). The formation of PML-independent MORC3-NBs relies on the ATPase activity, whereas colocalization with the PML bodies depends on MORC3 SUMOylation (Mimura et al., 2010). PML bodies, Cajal bodies, speckles, and other membraneless compartments are frequently observed in eukaryotic nuclei and are thought to be produced through phase separation (Banani et al., 2017; Hyman et al., 2014). These biomolecular condensates are typically micron scale in size, have liquid or gel-like properties, and allow for their components to be concentrated and be available for rapid multiple interactions.

Nuclear condensates and droplets formed through phase separation as a result of non-specific multivalent interactions are very dynamic and can sense and alter local chromatin environment (Shin et al., 2018). For example, liquid droplets of the heterochromatin protein 1 alpha (HP1α), induced by phosphorylation of this major chromatin compactor, stimulate rapid DNA condensation and formation of dense heterochromatin domains (Larson et al., 2017; Strom et al., 2017). A few proteins have been shown to phase separate into liquid condensates within low-density euchromatic regions and were proposed to mechanically push out chromatin (Boehning et al., 2018; Nair et al., 2019; Shin et al., 2018).

[1]Department of Pharmacology, University of Colorado School of Medicine, 12801 East 17th Avenue, Aurora, CO 80045, USA

[2]Department of Biology, Technische Universität Darmstadt, Darmstadt, 64287, Germany

[3]Department of Chemistry, University of Colorado, Denver, CO 80217, USA

[4]Lead Contact

*Correspondence: tatiana.kutateladze@ucdenver.edu

https://doi.org/10.1016/j.isci.2019.06.030

In this study, we report that MORC3 is capable of forming liquid-like nuclear condensates through phase separation. The number of MORC3-NBs decreases during cell division but is re-established in daughter cells. The ATPase activity drives phase separation *in vitro* and requires binding of MORC3 to DNA. Our findings highlight a previously uncharacterized mechanism by which the ATPase activity facilitates MORC3 liquid-liquid phase separation in the cell nucleus.

RESULTS AND DISCUSSION

MORC3 Forms Phase-Separated Condensates in Living Cells

MORC3 has been shown to associate with chromatin and form NBs (MORC3-NBs) in cells (Andrews et al., 2016; Li et al., 2016; Mimura et al., 2010). To gain insight into the nature and morphology of MORC3-NBs, we generated mCherry-tagged full-length MORC3 and visualized it in live HeLa cells stably expressing H2B-GFP (green fluorescent protein) by fluorescence microscopy (Figures 1A–1C). Throughout all experiments, three distinct patterns of mCherry-MORC3-NBs were observed in interphase (Figure S1). The majority of cells showed more than 30 small clusters, but some cells had a mixture of about 20 medium and small foci and a few cells displayed less than 10 foci with one or two being enlarged. All confocal microscopic images of MORC3-NBs demonstrated near-perfect rounded MORC3-NBs, indicative of liquid droplets (Figures 1A–1C and Video S1). This observation was consistent with previously reported immunostaining images of endogenous MORC3 (Mimura et al., 2010; Takahashi et al., 2007), supporting the notion that MORC3 forms NBs.

To characterize the physicochemical properties of MORC3-NBs, we measured the exchange kinetics of mCherry-MORC3 in selected foci by fluorescence recovery after photobleaching (FRAP) experiments. Cell images were collected at 10-s intervals for a duration of 270 s following the bleach, and changes in fluorescent signal of each bleached cluster were monitored (Figure 1D). The experiments were repeated on 10 MORC3-NBs, and an averaged signal intensity was normalized and plotted (Figure 1E). About 50% recovery of bleached fluorescence was observed within ~4.5 min after photobleaching, which suggested that mCherry-MORC3-NBs are viscous liquid droplets, characterized by rapid protein diffusion within the droplet and rapid exchange with surrounding environment. In further support, treatment of the cells with 1,6-hexanediol, known to selectively dissolve liquid droplets, resulted in complete disappearance of MORC3-NBs within 2 min (Figure 1F). Collectively, these data indicate that MORC3 forms nuclear condensates through liquid-liquid phase separation.

MORC3-NBs Heterogeneity Is Cell Cycle Dependent

To examine the phase separation capability of MORC3 over time, we carried out time-lapse live cell confocal microscopy experiments using live HeLa cells expressing mCherry-MORC3 and H2B-GFP. Figure 2 and Video S2 show a representative cell undergoing a complete cycle of cell division with cell images collected every 10 min. We observed drastic changes in the number and volume of MORC3-NBs between interphase and metaphase, which suggested that MORC3-NBs functioning is cell cycle dependent (Figures 2A and 2D). In interphase, 10–60 min prior entering mitosis, over 40 evenly distributed MORC3-NBs were counted in the nucleus of a cell, and these droplets localized primarily to the chromatin regions of low H2B density (Figure 2A, top panel, and Figure 2D). The number of MORC3-NBs decreased to two to three in metaphase, and notably these remaining MORC3-NBs were detached from the metaphase plate and chromatin (Figure 2A, middle panel, and Figure 2D). After mitosis was complete, the number and distribution of MORC3-NBs in the nuclei of daughter cells were faithfully re-established (Figure 2A, bottom panel, and Figure 2D). These data demonstrate that the number of MORC3-NBs decreases concomitantly with chromatin compaction, as indicated by H2B volume, and increases after nuclear division coinciding with chromatin decondensation (Figure 2B). Analysis of MORC3-NBs in nuclei from time-lapse data, shown in Figure 2C, illustrates a clear trend of cell cycle stage-dependent MORC3-NB heterogeneity.

MORC3 Phase Separates to Liquid Droplets upon Binding to DNA

We have previously shown that binding of the ATPase domain to DNA is necessary for the catalytic function of MORC3 (Andrews et al., 2016; Zhang et al., 2019a), and Mimura et al. reported that the formation of PML-independent MORC3-NBs relies on the ATPase activity (Mimura et al., 2010). We therefore asked whether the interaction with DNA could induce MORC3 phase separation. To test this idea, we examined the ability of the isolated ATPase domain, the ATPase-CW cassette, and the

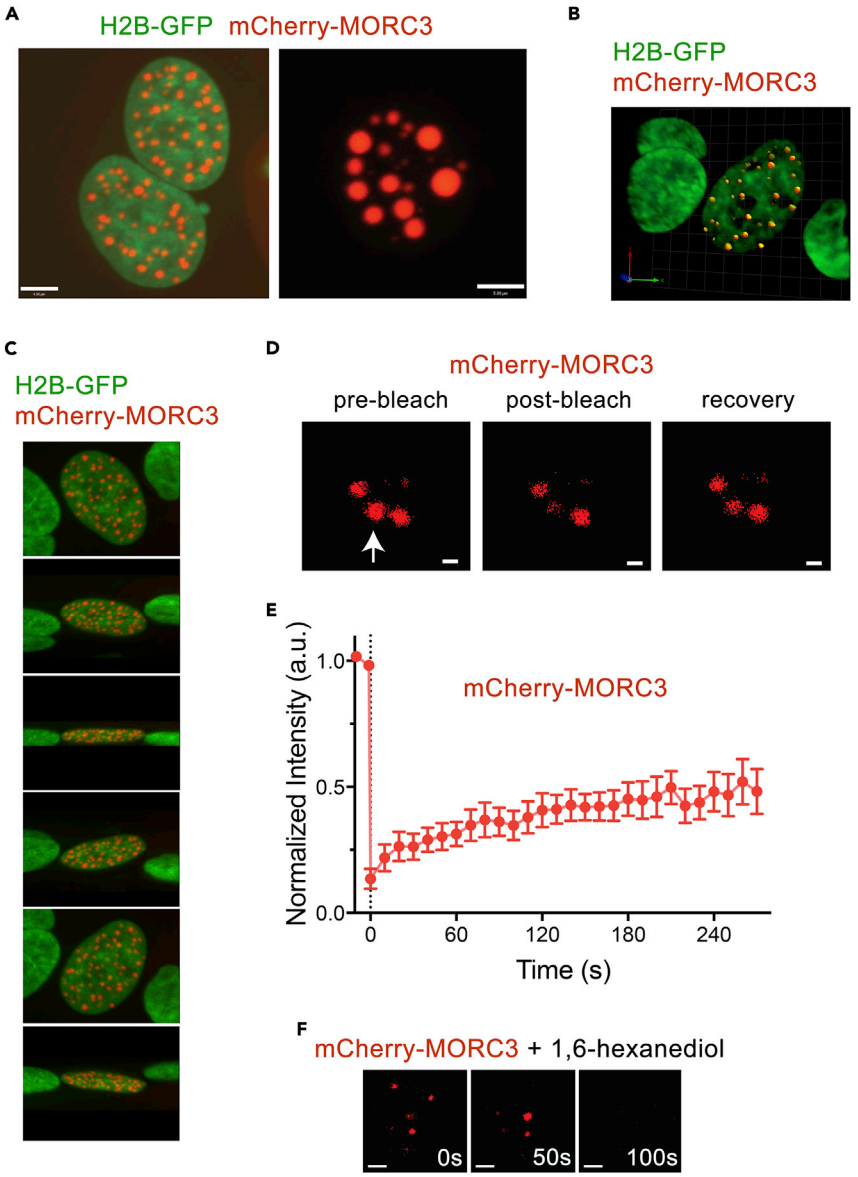

Figure 1. MORC3 Phase Separates to Condensates in Cells

(A–C) Representative fluorescence microscopy images of live HeLa cells expressing H2B-GFP (green) and MORC3 labeled with mCherry (red). Scale bar, 5 μm.

(D) Representative FRAP images of mCherry-MORC3 expressed in HeLa cells. The images were taken before (left) and after (middle and right) photobleaching. The condensate that was bleached is indicated by a white arrow. Scale bar, 2 μm.

(E) FRAP curve of mCherry-MORC3 NBs in HeLa cells. The FRAP curve was obtained from averaging data from 10 cells. Error bars represent SEM.

(F) Representative images of MORC3-NBs before and after treatment with 10% 1,6-hexanediol. Scale bar, 2 μm.

See also Figure S1 and Video S1.

C-terminal region of MORC3 to undergo phase separation *in vitro* (Figure S2). A clear solution of the recombinantly purified ATPase domain of MORC3 became visibly cloudy upon addition of 37-bp double-stranded DNA (Figure 3A). Visualizing the solution under a microscope revealed liquid-liquid separated droplets (Figure 3B). We note that this process is ATPase concentration dependent and that phase separation can be detected with naked eye when the ATPase concentration is above 13.3 μM (Figures 3C and S3).

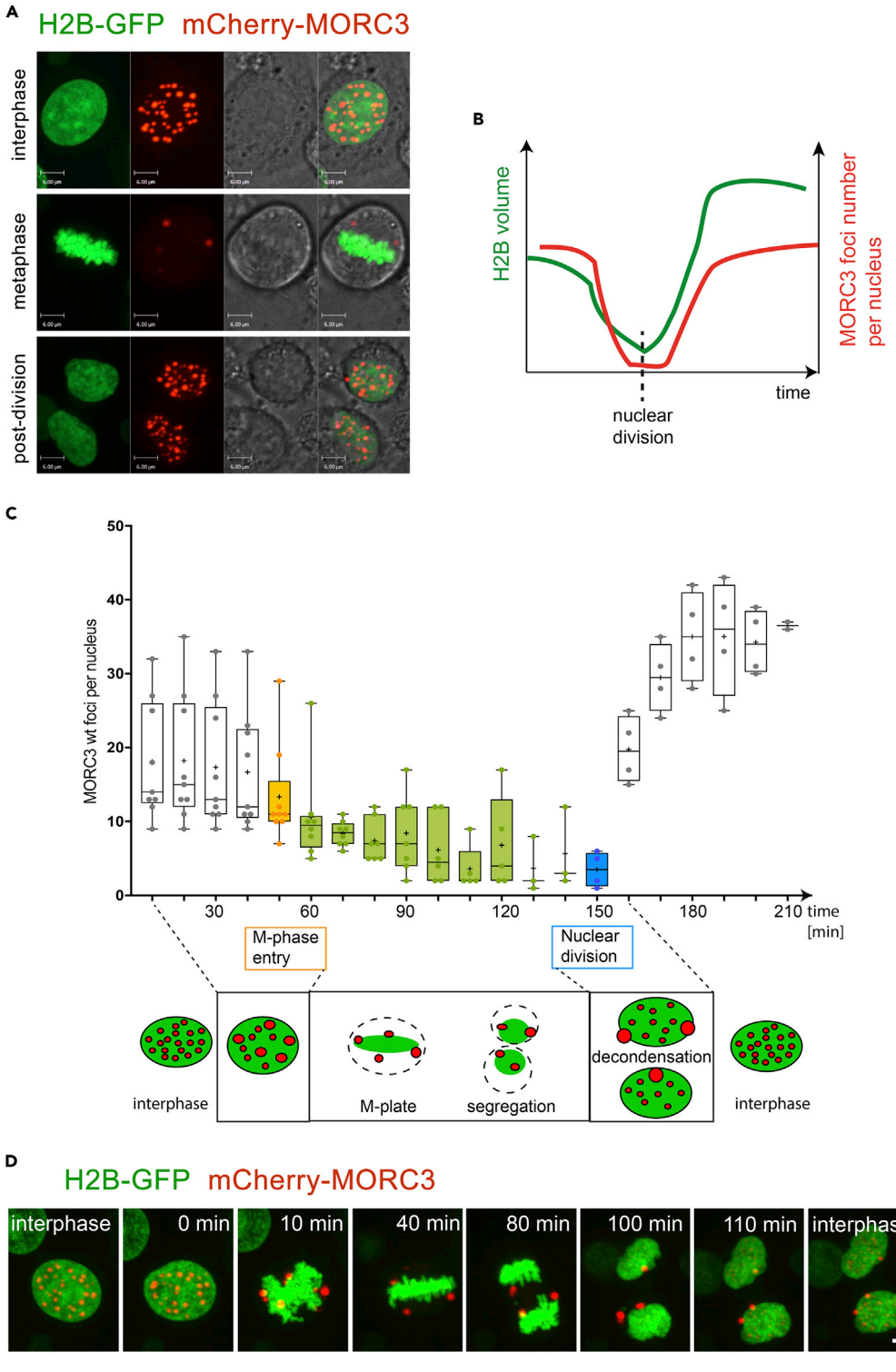

Figure 2. The Number of MORC3-NBs Changes during Cell Division

(A) A representative cell division with chromatin labeled with H2B-GFP (green) and MORC3 labeled with mCherry (red) visualized by confocal time-lapse microscopy in live cells. Foci numbers decrease in metaphase but recover to initial levels after cell division is complete. Scale bar, 6 μm.

(B) A plot of the changes of H2B volume (green) and MORC3 foci number (red) during cell division.

Figure 2. *Continued*

(C) Statistics and cartoon plots of the dynamic morphological change of MORC3-NBs after aligning cells to the entry point of mitosis.

(D) A representative cell division with chromatin labeled with H2B-GFP (green) and MORC3 labeled with mCherry (red) visualized by confocal time-lapse microscopy in live cells. Scale bar, 6 μm.

See also Figure S1 and Video S2.

To assess if the catalytic function of the MORC3 ATPase domain influences phase separation, we compared formation of condensates in the absence and presence of 2 mM ATP (Figure 3D). Addition of ATP to the ATPase domain greatly stimulated the formation of condensates. It was particularly evident when 147-bp 601 DNA and 37-bp DNA were used in the reactions, in which we observed an 8- to 9-fold increase in droplet counts (Figure 3D, red and orange bars). Considerably fewer droplets were formed upon addition of 15-bp DNA with or without ATP (Figure 3D, black bars). These results are consistent with our previous findings that the dimeric MORC3 ATPase domain cooperatively binds to 37-bp DNA but is incapable of the cooperative binding to the short 15-bp DNA (Zhang et al., 2019a). Furthermore, the ATPase phase separation was induced by AMPPNP, a non-hydrolysable ATP analog known to stabilize the ATPase dimer, but not by ADP (Figure 3E) (Li et al., 2016; Zhang et al., 2019a). Excess of DNA reversed the ATPase phase separation, likely indicating saturation of the DNA-binding sites and also pointing to a role of electrostatic interactions in the formation of condensates (Figures 3F and 3G).

Phase separation can facilitate cellular compartmentalization and increase local concentration of biomolecules, therefore, we postulated that DNA could be concentrated within the MORC3 droplets. We tested this hypothesis by a droplet formation assay using 37-bp fluorescein (FAM)-labeled DNA (Figure 3H). The MORC3 ATPase condensates, induced by FAM-DNA, showed strong fluorescent signal in confocal microscopy, but no condensates were formed by FAM-labeled DNA itself (Figure 3H). A nearly complete overlay of the FAM-DNA signal and MORC3 droplets implies that DNA was concentrated in the MORC3 condensates.

Phase Separation Requires Active MORC3

The DNA-binding function of the MORC3 ATPase domain is impeded by the adjacent CW domain in the MORC3 autoinhibited state, but the interaction of CW with histone H3 tail, either unmodified or H3K4me, releases autoinhibition (Andrews et al., 2016; Zhang et al., 2019a). To determine if the phase separation capability of MORC3 is also suppressed by CW, we tested the ATPase-CW cassette in *in vitro* condensate formation assays (Figure 4). As shown in Figures 4A and 4C, DNA or H3K4me3 peptide that was added individually to the ATPase-CW cassette failed to promote phase separation; however, addition of both DNA and H3K4me3 led to the formation of ATPase-CW liquid droplets (Figures 4A–4C). Furthermore, MORC3 ATPase-CW was able to concentrate FAM-labeled DNA only in the presence of the histone H3K4me3 peptide (Figure 4D). The mixture of unmodified H3 peptide and DNA also promoted ATPase-CW droplet formation, although to a lesser degree, which is in agreement with a 5-to-10-fold decrease in binding activity of CW toward non-methylated H3 (H3K4me0) (Andrews et al., 2016; Li et al., 2012, 2016; Liu et al., 2016) (Figures 4A and 4C). Importantly, MORC3 ATPase-CW phase separation was stimulated upon addition of the intact nucleosome, confirming the essential role of binding of CW to histone H3 tail, and therefore MORC3 activation in this process (Figure 4E).

Concluding Remarks

In this work, we show that MORC3 forms nuclear condensates through liquid-liquid phase separation that undergo substantial morphological changes in mitosis. The active state of the MORC3 ATPase-CW cassette drives phase separation, which requires concomitant binding of the ATPase domain to DNA and of the CW domain to histone H3 tail. In contrast, we found that the C-terminal region of MORC3, which is predicted to be mostly disordered, does not form liquid droplets itself, even at high protein concentration or upon incubation with DNA (data not shown). Our results further demonstrate that phase-separated MORC3 can concentrate free DNA within its droplets and, on the other hand, excess of DNA reduces the MORC3 droplet formation capability. Interestingly, the dynamic behavior of MORC3 condensates observed in mitosis is reminiscent of the behavior of PML NBs that co-accumulate several dozens of nuclear proteins (Dellaire et al., 2006). In future studies, it will be interesting to characterize and compare physicochemical properties of PML-dependent and PML-independent MORC3 NBs. It will also be important to

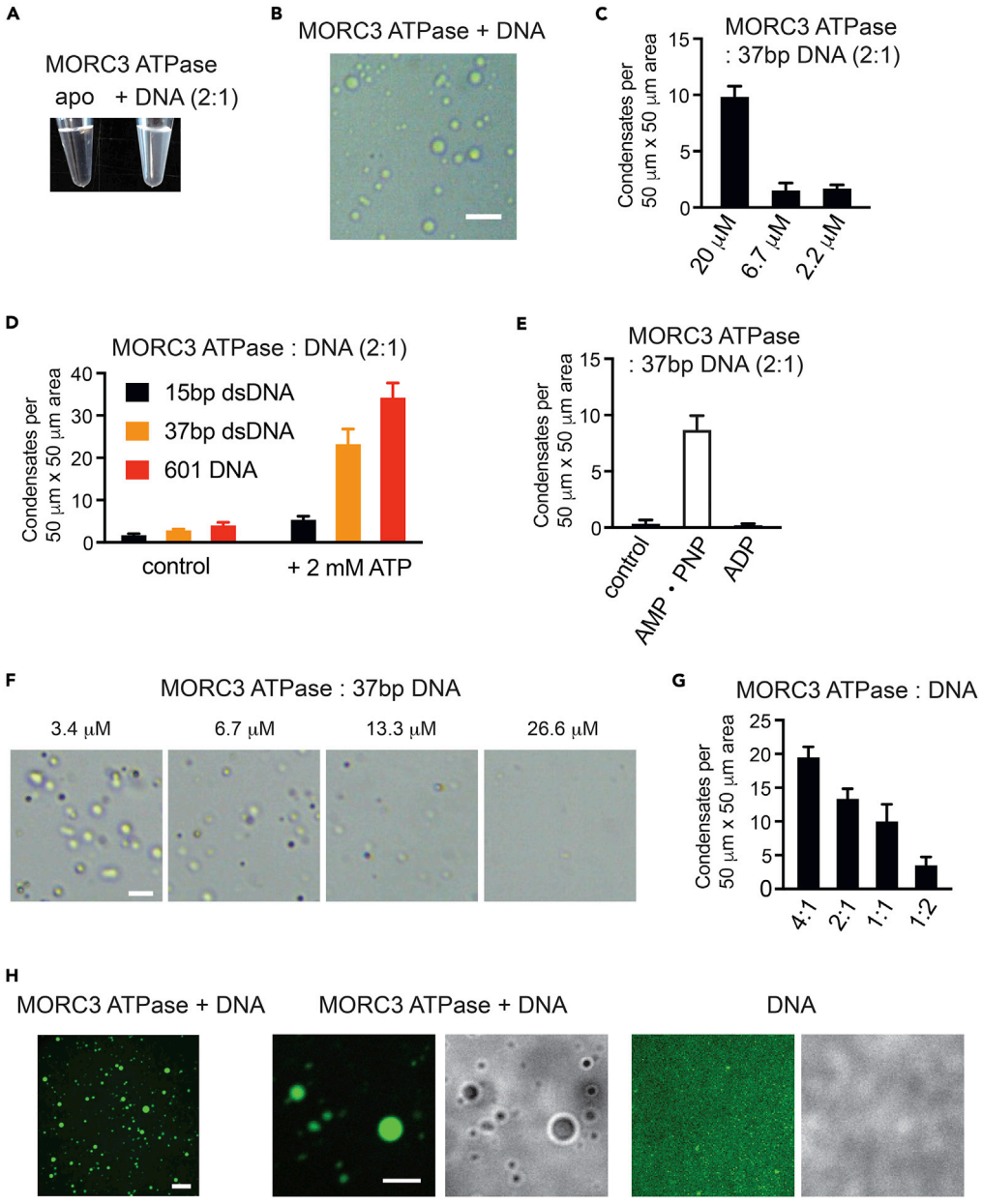

Figure 3. MORC3-ATPase Phase Separation Requires DNA

(A) Phase separation of 13.3 μM MORC3 ATPase with (right) or without (left) 6.7 μM 37-bp double-stranded (ds) DNA.

(B) A representative image of a sample containing 20 μM MORC3 ATPase and 10 μM 37-bp dsDNA on the surface of cover slides. Scale bar, 20 μm.

(C) Quantification of droplets counted in images acquired for indicated MORC3-ATPase concentrations.

(D) Quantification of MORC3-ATPase droplets in samples containing 13.3 μM MORC3 ATPase protein and 6.7 μM 15-bp dsDNA (black), 6.7 μM 37-bp dsDNA (orange), and 1.4 μM 601 DNA (red) without or with 2 mM ATP.

(E) Quantification of MORC3-ATPase droplets in samples containing 6.7 μM ATPase protein and 3.3 μM 37-bp dsDNA in the absence and presence of 2 mM AMPPNP and ADP.

(F) Representative images of 13.3 μM MORC3 ATPase with indicated amount of 37-bp dsDNA on the surface of cover slides. Scale bar, 10 μm.

(G) Quantification of (F).

(H) Representative confocal images of phase-separated MORC3-ATPase (13.3 μM) condensates (left and middle) or buffer with FAM-labeled DNA (6.7 μM) (right). Scale bar, 20 μm (left) and 10 μm (middle and right). Number of droplets were counted in a 50 × 50-μm square region (C, D, E, and G). For each sample, six square regions were counted. Error bars represent SEM. See also Figures S2 and S3.

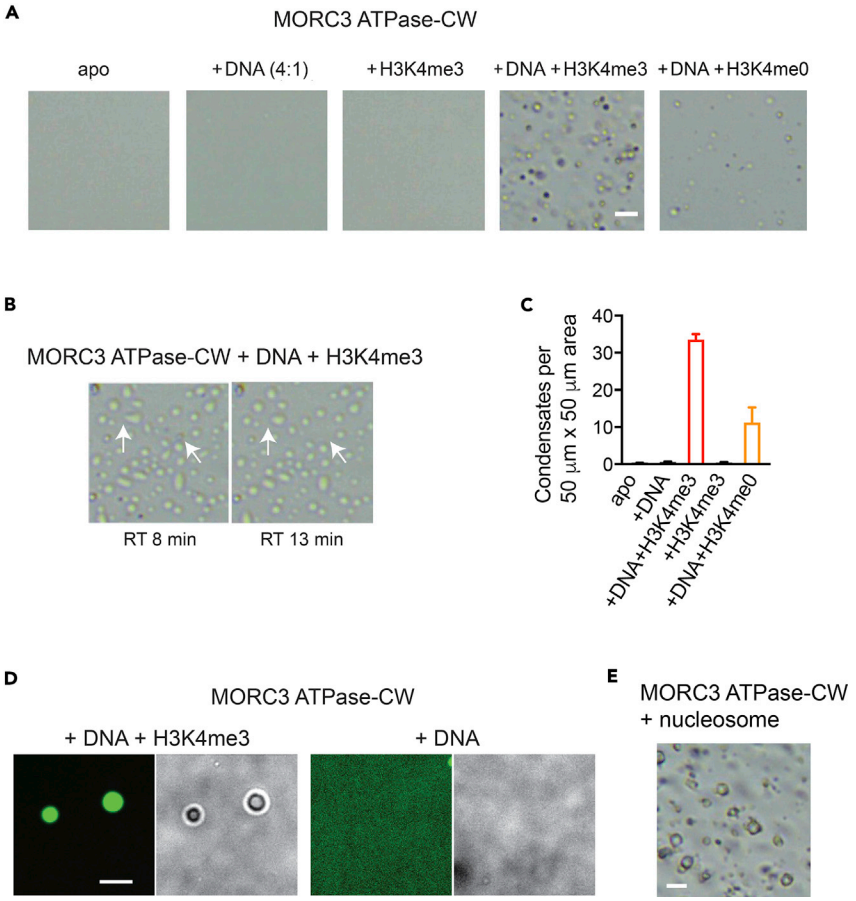

Figure 4. Phase Separation of MORC3 Is Impeded by the CW Domain

(A and B) Representative images of MORC3 ATPase-CW (20 μM) with or without 37-bp double-stranded DNA (5 μM) and histone H3K4me0 (1–12) and H3K4me3 (1–12) peptides (200 μM) on the surface of cover slides. Scale bar, 10 μm. As the MORC3 ATPase-CW condensates settled on the glass slide, droplets with irregular shapes gradually became spherical while small droplets fused together, as indicated by arrows in (B).

(C) Quantification of (A). Number of droplets was counted in a 50 × 50-μm square region. For each sample, six square regions were counted. Error bars represent SEM.

(D) Representative confocal images of phase-separated MORC3 ATPase-CW (20 μM) condensates in the presence of 6.7 μM FAM-labeled DNA and 200 μM H3K4me3 peptide (left). No condensates are detected without H3K4me3 peptide (right). Scale bar, 10 μm. See also Figure S2.

(E) Representative images of MORC3 ATPase-CW (20 μM) incubated with reconstituted unmodified nucleosome (10 μM) on the surface of cover slides. Scale bar, 10 μm.

determine the composition of MORC3-NBs in different cell cycle stages and examine whether other proteins can be recruited to MORC3-NBs.

Limitations of the Study

In this study, we overexpressed fluorescently labeled mCherry-MORC3 necessary for FRAP experiment in live HeLa cells. To fully characterize the morphological changes and phase separation properties of MORC3, studies using genome-edited cells expressing fluorescently tagged endogenous MORC3 may be considered.

METHODS

All methods can be found in the accompanying Transparent Methods supplemental file.

SUPPLEMENTAL INFORMATION

Supplemental Information can be found online at https://doi.org/10.1016/j.isci.2019.06.030.

ACKNOWLEDGMENTS

We thank Anne Lehmkuhl for helping with experiments. This work was supported by grants from NIH GM106416, GM125195 and GM100907 to T.G.K. and from German Research Foundation DFG CA198/9-2 and German Federal Ministry of Education and Research (BMBF) GREWIS 02NUK017D to M.C.C. A.H.T. is an American Heart Association postdoctoral fellow.

AUTHOR CONTRIBUTIONS

Y.Z., B.B., A.H.T, X.R., G.M.W. and J.B. performed experiments and together with M.C.C. and T.G.K. analyzed the data. Y.Z. and T.G.K. wrote the manuscript with input from all authors.

DECLARATION OF INTERESTS

The authors declare no competing interests.

Received: April 11, 2019
Revised: June 3, 2019
Accepted: June 19, 2019
Published: July 26, 2019

REFERENCES

Andrews, F.H., Tong, Q., Sullivan, K.D., Cornett, E.M., Zhang, Y., Ali, M., Ahn, J., Pandey, A., Guo, A.H., Strahl, B.D., et al. (2016). Multivalent chromatin engagement and inter-domain crosstalk regulate MORC3 ATPase. Cell Rep. *16*, 3195–3207.

Banani, S.F., Lee, H.O., Hyman, A.A., and Rosen, M.K. (2017). Biomolecular condensates: organizers of cellular biochemistry. Nat. Rev. Mol. Cell. Biol. *18*, 285–298.

Boehning, M., Dugast-Darzacq, C., Rankovic, M., Hansen, A.S., Yu, T., Marie-Nelly, H., McSwiggen, D.T., Kokic, G., Dailey, G.M., Cramer, P., et al. (2018). RNA polymerase II clustering through carboxy-terminal domain phase separation. Nat. Struct. Mol. Biol. *25*, 833–840.

Dellaire, G., Eskiw, C.H., Dehghani, H., Ching, R.W., and Bazett-Jones, D.P. (2006). Mitotic accumulations of PML protein contribute to the re-establishment of PML nuclear bodies in G1. J. Cell Sci. *119*, 1034–1042.

Gonzalez-Fernandez, R., Morales, M., Avila, J., and Martin-Vasallo, P. (2012). Changes in leukocyte gene expression profiles induced by antineoplastic chemotherapy. Oncol. Lett. *3*, 1341–1349.

Gunawardena, H., Wedderburn, L.R., Chinoy, H., Betteridge, Z.E., North, J., Ollier, W.E., Cooper, R.G., Oddis, C.V., Ramanan, A.V., Davidson, J.E., et al. (2009). Autoantibodies to a 140-kd protein in juvenile dermatomyositis are associated with calcinosis. Arthritis Rheum. *60*, 1807–1814.

Hyman, A.A., Weber, C.A., and Julicher, F. (2014). Liquid-liquid phase separation in biology. Annu. Rev. Cell Dev. Biol. *30*, 39–58.

Larson, A.G., Elnatan, D., Keenen, M.M., Trnka, M.J., Johnston, J.B., Burlingame, A.L., Agard, D.A., Redding, S., and Narlikar, G.J. (2017). Liquid droplet formation by HP1alpha suggests a role for phase separation in heterochromatin. Nature *547*, 236–240.

Li, S., Yen, L., Pastor, W.A., Johnston, J.B., Du, J., Shew, C.J., Liu, W., Ho, J., Stender, B., Clark, A.T., et al. (2016). Mouse MORC3 is a GHKL ATPase that localizes to H3K4me3 marked chromatin. Proc. Natl. Acad. Sci. U S A *113*, E5108–E5116.

Li, X., Foley, E.A., Molloy, K.R., Li, Y., Chait, B.T., and Kapoor, T.M. (2012). Quantitative chemical proteomics approach to identify post-translational modification-mediated protein-protein interactions. J. Am. Chem. Soc. *134*, 1982–1985.

Liu, Y., Tempel, W., Zhang, Q., Liang, X., Loppnau, P., Qin, S., and Min, J. (2016). Family-wide characterization of histone binding abilities of human CW domain containing proteins. J. Biol. Chem. *291*, 9000–9013.

Mimura, Y., Takahashi, K., Kawata, K., Akazawa, T., and Inoue, N. (2010). Two-step colocalization of MORC3 with PML nuclear bodies. J. Cell Sci. *123*, 2014–2024.

Nair, S.J., Yang, L., Meluzzi, D., Oh, S., Yang, F., Friedman, M.J., Wang, S., Suter, T., Alshareedah, I., Gamliel, A., et al. (2019). Phase separation of ligand-activated enhancers licenses cooperative chromosomal enhancer assembly. Nat. Struct. Mol. Biol. *26*, 193–203.

Shin, Y., Chang, Y.C., Lee, D.S.W., Berry, J., Sanders, D.W., Ronceray, P., Wingreen, N.S., Haataja, M., and Brangwynne, C.P. (2018). Liquid nuclear condensates mechanically sense and restructure the genome. Cell *175*, 1481–1491.e13.

Sloan, E., Orr, A., and Everett, R.D. (2016). MORC3, a component of PML nuclear bodies, has a role in restricting herpes simplex virus 1 and human cytomegalovirus. J. Virol. *90*, 8621–8633.

Strom, A.R., Emelyanov, A.V., Mir, M., Fyodorov, D.V., Darzacq, X., and Karpen, G.H. (2017). Phase separation drives heterochromatin domain formation. Nature *547*, 241–245.

Takahashi, K., Yoshida, N., Murakami, N., Kawata, K., Ishizaki, H., Tanaka-Okamoto, M., Miyoshi, J., Zinn, A.R., Shime, H., and Inoue, N. (2007). Dynamic regulation of p53 subnuclear localization and senescence by MORC3. Mol. Biol. Cell *18*, 1701–1709.

Ver, L.S., Marcos-Villar, L., Landeras-Bueno, S., Nieto, A., and Ortin, J. (2015). The cellular factor NXP2/MORC3 is a positive regulator of influenza virus multiplication. J. Virol. *89*, 10023–10030.

Zhang, Y., Klein, B.J., Cox, K.L., Bertulat, B., Tencer, A.H., Holden, M.R., Wright, G.M., Black, J., Cardoso, M.C., Poirier, M.G., et al. (2019a). Mechanism for autoinhibition and activation of the MORC3 ATPase. Proc. Natl. Acad. Sci. U S A. https://doi.org/10.1073/pnas.1819524116.

Zhang, Y., Ahn, J., Green, K.J., Vann, K.R., Black, J., Brooke, C.B., and Kutateladze, T.G. (2019b). MORC3 is a target of the Influenza A viral protein NS1. Structure *27*, 1029–1033.e3.

ISCI, Volume *17*

Supplemental Information

MORC3 Forms Nuclear Condensates through Phase Separation

Yi Zhang, Bianca Bertulat, Adam H. Tencer, Xiaojun Ren, Gregory M. Wright, Joshua Black, M. Cristina Cardoso, and Tatiana G. Kutateladze

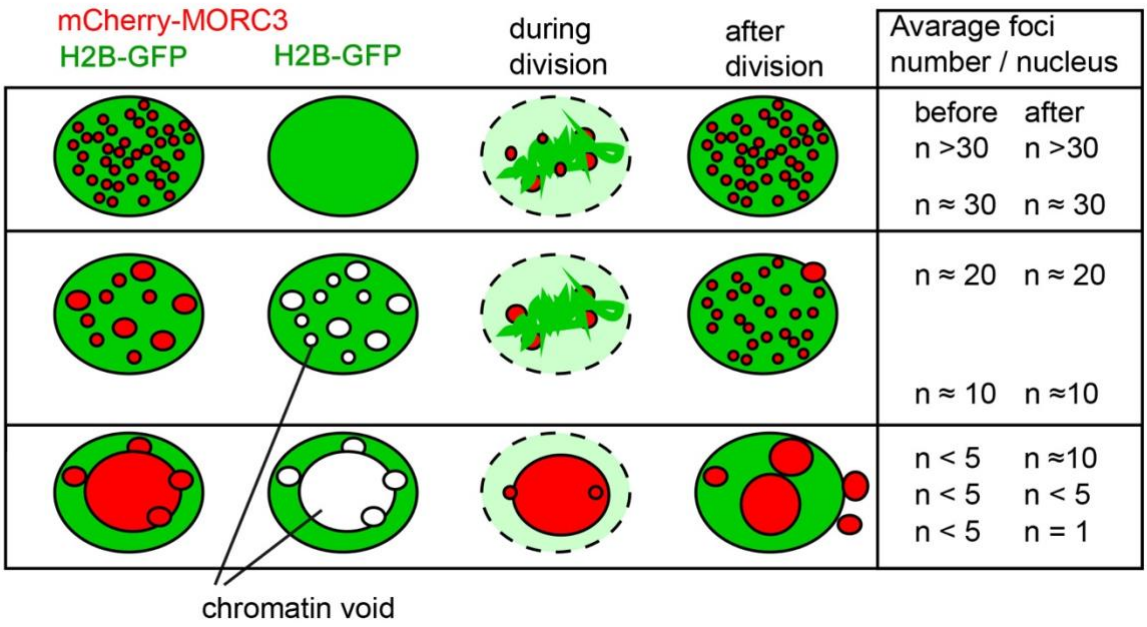

Figure S1. MORC3-NBs show distinct foci pattern in cells, Related to Figures 1 and 2. In over 8 independent transient transfection experiments, the depicted foci patterns were observed regularly in similar proportions. The vast majority of cells demonstrated more than 30 small foci per nucleus, followed by a large fraction of cells with medium and small foci and a minority of cells with less than 5 and 1-2 very large foci. Live cell DNA counterstaining experiments revealed an exclusion of DNA/chromatin and MORC3 signals in medium and large foci.

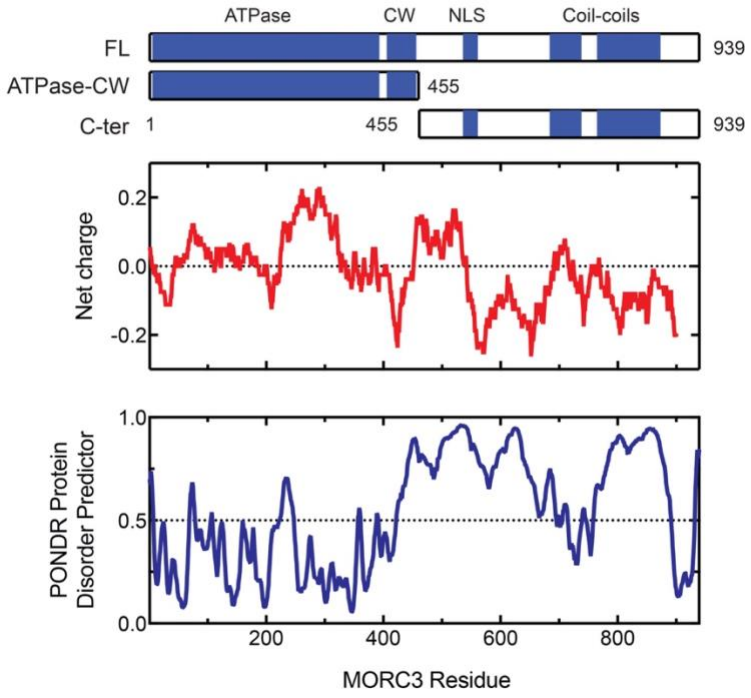

Figure S2. Domain structure, net charge, and disorder tendency of human MORC3 protein, Related to Figures 3 and 4. The net charge was calculated and plotted using a sliding window of 40 amino acids by EMBOSS. The disorder tendency was predicted using PONDR software. A score greater than 0.5 indicates intrinsically disordered regions.

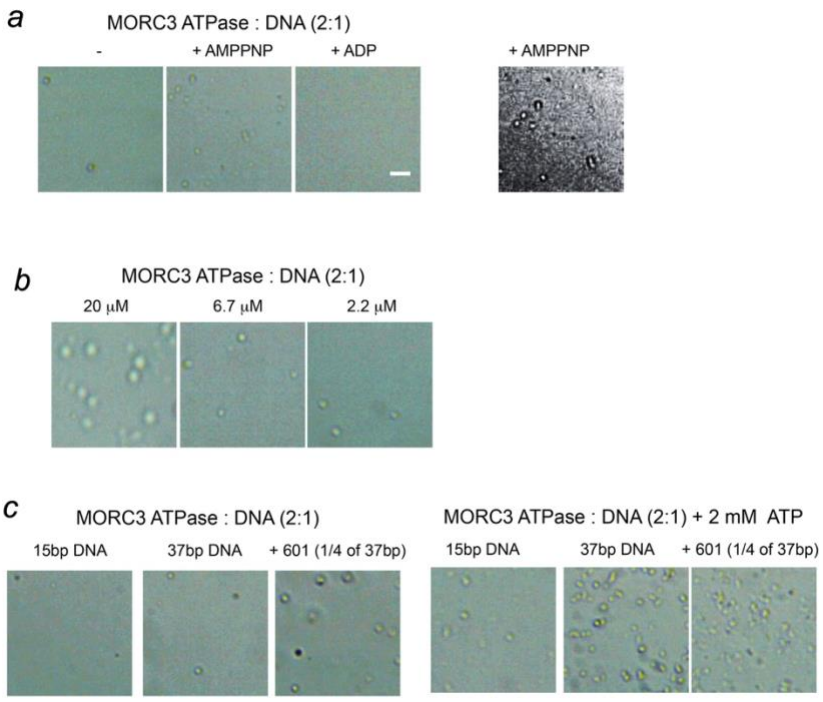

Figure S3. Representative images of MORC3-ATPase condensates, Related to Figure 3.

(a) Representative images of samples containing 6.7 μM ATPase protein and 3.3 μM 37 bp dsDNA in the absence and presence of 2 mM AMPPNP and ADP. Scale bar, 10 μm. A representative image processed by Photoshop for counting droplets is shown on the right. (b) Representative images acquired for indicated MORC3-ATPase concentrations with a fixed protein:DNA ratio of 2:1. (c) Representative images of samples containing 13.3 μM ATPase protein and 6.7 μM 15 bp dsDNA, 6.7 μM 37 bp dsDNA and 1.4 μM 601 DNA without or with 2 mM ATP.

TRANSPARENT METHODS

Cells, DNA Constructs and Transfection

Live cell experiments were performed with HeLa-H2B-GFP cells (Kanda et al., 1998), as previously described (Martin and Cardoso, 2010). Cells were cultivated using standard cell culture conditions (37 °C, 5% CO_2, humidified atmosphere) in D-MEM (Sigma-Aldrich) supplemented with 10% v/v FCS (Gibco), 2 mM glutamine (Sigma-Aldrich) and 50 µg/µl gentamycin (Sigma-Aldrich). If not stated otherwise, transient transfections with N-terminal mCherry-fused *MORC3* were performed with the Neon Transfection System (Invitrogen). The mCherry-MORC3 plasmid was generated using previously reported FLAG-tagged MORC3 plasmid by substituting the FLAG tag sequence with mCherry coding sequence through double digestion and T4 ligation (Andrews et al., 2016). HeLa-H2B-GFP cells were cultured in 10 cm petri dishes to 80% confluence, trypsin treated and harvested in PBS (centrifugation at 300 xg for 5 min). The resulting pellets were suspended according to manufacturer's instructions and transfected using 2-10 µg plasmid DNA and a 100 µl Neon tip. After electroporation, 100 µl were equally distributed to 3.5 mm glass bottom Ibidi dishes. Cells were allowed to recover at standard cell culture conditions (37 °C, 5% CO, humidified) overnight. The following day media was exchanged, and transfection efficiency was estimated by fluorescent light microscopy.

Image Acquisition and Analysis

Live cell time-lapse microscopy was performed using an UltraView VoX spinning disk system mounted on an inverted Nikon Ti-E microscope. Z-stack images were taken with a 60x plan apochromat NA 1.45 objective (Nikon; Tokyo, Japan) and a cooled 14-bit EMCCD camera (C9100-50, Hamamatsu Photonics K.K.; Hamamatsu City, Japan) yielding a voxel size of xyz 0.123 µm x 0.122 µm x 0.5 µm. If not stated otherwise, time lapse movies were generated with at a time interval of 10 min. Images and movies were analyzed and processed with the Perkin Elmer software "Volocity 6.3".

For imaging over time, individual nuclei were separated by cropping to a user defined region of interest. Quality parameters for nuclei selection were a completely covered nucleus in z and cell viability (checked in transmission light by general morphologic appearance) throughout the acquisition time. Within the selected regions of interest (ROIs), interphase nuclei were first segmented using H2B-GFP signals and potential holes inside the nucleus were filled to generate a solid chromatin volume object. MORC3-mCherry foci were identified and segmented either automatically or by intensity and assigned to tracked nuclei. The resulting measurement routine yielded MORC3 foci numbers per time point. All generated values were subsequently exported for processing in excel (Microsoft) and Prism 7 (GraphPad). For comparison of MORC3 foci numbers, first movie frames were assigned to landmarks such as metaphase entry and telophase and the respective MORC3 foci values were analyzed using Excel and Prism 7.

Fluorescence recovery after photobleaching (FRAP) experiments

WT mCherry-MORC3 plasmid were transfected into 2 million HeLa cells in 10-cm-diameter tissue culture dish by Lipofectamine 3000 (Life Technology, L3000-075) using manufacturer instructions. The next day after transfection, cells were trypsinized, harvested, seeded to a 35 mm gelatin-coated coverglass-bottom dish and cultured overnight. Cell culture medium was replaced with the live-cell imaging medium and maintained at 37 °C using a heater controller. FRAP imaging was performed using a Zeiss LSM 700 Observer as described previously (Tatavosian et al., 2019). Briefly, two images were taken before photobleaching and 20 images were taken with 10s intervals immediately after photobleaching. The images were analyzed using ImageJ. Fluorescence intensities were normalized to the signal before photobleaching to obtain the fluorescence recovery.

Protein expression and purification

The human MORC3 ATPase (aa 1-392) and ATPase-CW (aa 1-455) proteins were expressed and purified as described previously (Zhang, 2019). The C-terminus of MORC3 (aa 455-939) was cloned into a pDEST-17 vector and expressed and purified as the ATPase domain.

In vitro condensate formation

All in vitro condensate formation assays were performed in a buffer containing 20 mM Tris-HCl (pH 7.5), 50 mM NaCl, 1 mM $MgSO_4$ and 1 mM DTT. All samples were prepared on ice and incubated for approximately 5 min before imaging on siliconized glass cover slides (Hampton). For MORC3 ATPase-CW, 20 μM protein samples were parallelly prepared, with or without 5 μM 37bp dsDNA, 200 μM histone H3K4me0 (1-12) or H3K4me3 (1-12) peptide and 10 μM reconstituted unmodified nucleosome. For MORC3 ATPase, unless otherwise stated, samples were prepared with or without 37 bp dsDNA at a protein:DNA ratio of 2:1 (see also figure 3 legends). Microscopy of the droplets was done using an M150C-I microscope (AmScope) equipped with a 10× objective and a MD35 digital camera (AmScope). A microscope camera calibration slide (OMAX, 0.01mm) was used to determine the scale. The number of condensates was counted in a 50 μm × 50 μm square area. Six non-overlapping square regions were counted for each sample and plotted with Prism 7.

To prepare MORC3 condensates that concentrate DNA, 13.3 μM ATPase or 20 μM ATPase-CW was mixed with 6.7 μM fluorescein (FAM)-labeled 37 bp dsDNA. For ATPase-CW, one sample was supplemented with 200 μM histone H3K4me3 (1-12) peptide. Confocal images were acquired on a Zeiss Observer.Z1 inverted microscope using a 40× oil objective and digitally captured. For the excitation and emission of FAM, a 488 nm laser was used. Images were processed and presented using ImageJ and Photoshop.

REFERENCES

Kanda, T., Sullivan, K.F., and Wahl, G.M. (1998). Histone-GFP fusion protein enables sensitive analysis of chromosome dynamics in living mammalian cells. Current biology : CB *8*, 377-385.
Martin, R.M., and Cardoso, M.C. (2010). Chromatin condensation modulates access and binding of nuclear proteins. FASEB J *24*, 1066-1072.
Tatavosian, R., Kent, S., Brown, K., Yao, T., Duc, H.N., Huynh, T.N., Zhen, C.Y., Ma, B., Wang, H., and Ren, X. (2019). Nuclear condensates of the Polycomb protein chromobox 2 (CBX2) assemble through phase separation. The Journal of biological chemistry *294*, 1451-1463.
Zhang, Y.e.a. (2019). MORC3 is a target of the Influenza A viral protein NS1. Structure.